

# Deformation and Shrinkage Effects on the Soil Water Release Characteristic

**Andrew S. Gregory\***

**Nigel R. A. Bird**

**W. Richard Whalley**

Cross-Institute Programme for  
Sustainable Soil Function  
Dep. of Soil Science  
Rothamsted Research  
Harpenden, Hertfordshire AL5 2JQ, UK

**G. Peter Matthews**

Environmental and Fluid Modelling Group  
Univ. of Plymouth  
Drake Circus  
Plymouth PL4 8AA, UK

**Iain M. Young**

SIMBIOS Centre  
Univ. of Abertay  
Bell St.  
Dundee DD1 1HG, UK

currently at  
School of Environmental and Rural Science  
Univ. of New England  
Armidale, NSW 2351, Australia

The soil water release characteristic is controlled by the soil pores and so alteration of the pore system will have an effect. We sought to examine the effects of various pore deformations in a range of arable and grassland soils from the UK. Sieved topsoil materials were compressed to 50 or 200 kPa, or remolded to simulate shear deformation at the plastic limit. They were then subjected to matric potentials from 0 to -1500 kPa using conventional tension and pressure plate apparatus. Volume changes were monitored to assess shrinkage. Further samples in the compressed state were subjected to x-ray computed tomography scanning to nondestructively characterize the soil pore system. Increasing the compression from 50 to 200 kPa mainly affected the >30- $\mu\text{m}$  pores, changing a dual porous system of inter- and intraaggregate pores to one mainly dominated by intraaggregate pores, as confirmed by gravimetric water release characteristic data and the scans. Shear-deformed soils retained more water than the compressed soil and shrank more, such that they remained tension saturated at low (negative) matric potentials. We developed a function to predict the soil saturation state as a function of matric potential and porosity. This explained 28 to 63% of the variance, irrespective of the initial structural state, but up to 94% of the variation when one of the fitted parameters was allowed to vary for the different initial states. This was sufficiently systematic to suggest that a general model of the effects of soil deformation and shrinkage on the water release characteristic may be possible.

**Abbreviations:** CT, (x-ray) computed tomography; H, 200-kPa (high) compression treatment; L, 50-kPa (low) compression treatment; OM, organic matter;  $R^2_{\text{adj}}$ , proportion of the variance accounted for; S, shear deformed treatment.

The soil water release characteristic is an important soil physical property controlled by the soil pores. If the pore geometry is deformed by external perturbations, such as compaction or shear, then this will affect water retention (Wu et al., 1997; Richard et al., 2001; Tarantino and Tombolato, 2005; Dexter et al., 2008; Gregory et al., 2009; Li and Zhang, 2009; Matthews et al., 2010). In most soils there is also a decrease in the pore volume associated with water release as the soil shrinks (Simms and Yanful, 2001; Braudeau et al., 2005; Whalley et al., 2008; Li and Zhang, 2009). Both deformation and shrinkage have important implications for soil physical functioning. The loss of larger pores by deformation may cause drainage problems (Matthews et al., 2010). Shrinking soils may increase in strength (Whalley et al., 2008) and may remain largely saturated at negative matric potentials as water is released. In the most extreme case, the decrease in the soil pore volume is equal to the loss of water, defined as normal shrinkage (Haines, 1923), and the soil remains saturated under tension.

Newman and Thomasson (1979) reported a general link between the initial proportion of <0.2- $\mu\text{m}$  pores and normal shrinkage. They also suggested that in some less-stable soils, pores up to 30  $\mu\text{m}$  in size contracted on drying, a finding that led them to conclude that in clay soils, much plant-available water is supplied by shrinkage rather than emptying of pores. Li and Zhang (2009) also linked shrinkage of pores >0.3  $\mu\text{m}$  with water release. Others have also suggested that normal shrinkage is controlled by the intraaggregate pores (Bronswijk, 1991; Cabidoche and Ozier-Lafontaine, 1995; Braudeau et al., 2005).

Soil Sci. Soc. Am. J. 74:1104–1112

Published online 9 Apr. 2010

doi:10.2136/sssaj2009.0278

Received 24 July 2009.

\*Corresponding author (andy.gregory@bbsrc.ac.uk).

© Soil Science Society of America, 677 S. Segoe Rd., Madison WI 53711 USA

All rights reserved. No part of this periodical may be reproduced or transmitted in any form or by any means, electronic or mechanical, including photocopying, recording, or any information storage and retrieval system, without permission in writing from the publisher. Permission for printing and for reprinting the material contained herein has been obtained by the publisher.

While there are many models of the soil water release characteristic, most assume rigidity and do not account for volume change during measurement (e.g., van Genuchten, 1980). Although this assumption simplifies the subsequent prediction of other hydraulic properties, such as unsaturated hydraulic conductivity (Mualem, 1976), such an approach does not capture the complexity of the shrinkage process that occurs in many soils. Kim et al. (1999) developed separate models to predict volume change and unsaturated water flow, linked to soil water release in swelling materials. Li and Zhang (2009) developed models of pore size distributions predicted from changes in porosity caused by different mechanisms. More recently, Gallipoli et al. (2003) extended the van Genuchten model to allow for volume change in a porous material. This is a very useful framework for describing the processes more realistically.

In this study, we examined the effect of deformation on shrinkage and the soil water release characteristic of a range of arable and grassland agricultural soils from the UK. We assessed the effect of the initial condition on shrinkage and sought to devise a model that could relate matric potential, porosity, and the degree of saturation for all initial structural conditions for each soil, following the approach of Gallipoli et al. (2003). We also made use of x-ray computed tomography (CT) image analysis to assess the effect of deformation.

## MATERIALS AND METHODS

### Soils

Surface soil samples were collected from three arable sites and three grassland sites in the UK (Table 1). Arable soils were collected from the inorganic fertilizer [(P)KMg] and farmyard manure (FYM) treatments of the Broadbalk experiment at Rothamsted Research in Hertfordshire.

These soils were chosen because they are essentially identical except for the soil organic matter (OM) contents, which reflect their long-term management history. The third arable soil was collected from Warren field at the Woburn Experimental Farm in Bedfordshire, which is more representative of arable agriculture in southeast England. One of the grassland soils, Highfield, was also collected from Rothamsted. This was taken from a long-term cut grassland field and has developed from the same parent material as the Broadbalk soils. The remaining two grassland soils, Rowden and Bridestowe, were collected from two sites in Devon that reflect typical grazed grassland agriculture in southwest England. Most of the six soils approximated to either the Paleudalf or Hapludalf Great Groups in the U.S. Soil Taxonomy (Avery, 1980) and were loamy in texture. The exception was the Rowden soil, which had a greater clay content and approximated a Haplaquept (Avery, 1980). All soils were crumbled to pass a 4-mm-aperture sieve and left to air dry in a bulk sample.

### Water Content–Consolidation Characteristic

An initial experiment was conducted to find the appropriate water contents to prepare the soils before creating the initial structural states. Air-dry soil was wetted to a range of water contents and subjected to a confined uniaxial compression of 200 kPa to fill a cylindrical core (54-mm i.d., 25-mm height) before oven drying at 105°C for 48 h. The water content–dry bulk density relationship was plotted and a second-order polynomial function was fitted. The water content associated with the maximum density was derived.

### Sample Preparation

The air-dry soil samples were wetted to the water contents that gave the maximum bulk density (see above) and equilibrated in air-tight

**Table 1. Selected properties of the six soils from the UK.**

Property	Broadbalk (P)KMg	Broadbalk FYM	Warren	Rowden	Bridestowe	Highfield
Location	Rothamsted Res., Hertfordshire	Rothamsted Res., Hertfordshire	Woburn Exp. Farm, Bedfordshire	North Wyke Res., Devon	Bridestowe, Devon	Rothamsted Res., Hertfordshire
Grid reference						
GB national grid	TL121134	TL121134	SP968364	SX652994	SX512873	TL129130
Latitude	51°48'36" N	51°48'36" N	52°01'06" N	50°46'42" N	50°39'55" N	51°48'18" N
Longitude	0°22'30" W	0°22'30" W	0°35'30" W	3°54'54" W	4°07'03" W	0°21'48" W
Soil type						
SSEW† group‡	Paleo-argillic brown earth	Paleo-argillic brown earth	Brown earth	Stagnogley soil	Brown earth	Paleo-argillic brown earth
SSEW† series§	Batcombe	Batcombe	Flitwick	Hallsworth	Denbigh	Batcombe
FAO¶ #	Chromic Luvisol	Chromic Luvisol	Dystric Cambisol	Gleyic Luvisol	Dystric Cambisol	Chromic Luvisol
U.S. Soil Taxonomy##	Paleudalf	Paleudalf	Hapludalf	Haplaquept	Hapludalf	Paleudalf
Land use	Arable, cereals, fertilized	Arable, cereals, farmyard manure	Arable, cereals, beans	Grass, unfertilized, grazed	Grass, unfertilized, grazed	Grass, unfertilized, cut
Sand (2000–63 µm), kg kg <sup>-1</sup> dry soil	0.252	0.252	0.538	0.147	0.186	0.179
Silt (63–2 µm), kg kg <sup>-1</sup> dry soil	0.497	0.497	0.203	0.396	0.460	0.487
Clay (<2 µm), kg kg <sup>-1</sup> dry soil	0.252	0.252	0.260	0.457	0.354	0.333
Texture, SSEW† class‡	clay loam	clay loam	sandy clay loam	clay	silty clay	silty clay loam
Particle density, g cm <sup>-3</sup>	2.560	2.508	2.587	2.439	2.480	2.436
Organic matter, kg kg <sup>-1</sup> dry soil	0.023	0.060	0.038	0.138	0.065	0.089
Water content for packing, kg kg <sup>-1</sup> dry soil	0.26	0.28	0.27	0.58	0.40	0.37

† Soil Survey of England and Wales classification system.

‡ Avery (1980).

§ Clayden and Hollis (1984).

¶ World Reference Base for Soil Resources.

# Approximation.

containers at 4°C for at least 48 h. The wetted soil was packed into cylindrical plastic cores (50-mm i.d., 25-mm height) to three initial structural conditions. Soil was either uniaxially compressed to 50 or 200 kPa, filled incrementally in approximately five layers while radially confined in the cores, or was wetted further to just above the plastic limit and remolded into the cores using a spatula. These treatments simulated consolidation and shear deformation, respectively. They are hereafter termed L, H, and S for low compression (50 kPa), high compression (200 kPa), and shear deformation, respectively. The sample preparation method outlined above was highly reproducible in terms of the initial total porosity created for each of the 18 soil–treatment combinations (standard deviation [ $n = 14–21$ ] of 0.005–0.030).

For each of the 18 treatments (soil  $\times$  structural condition), two types of core were prepared. One type was prepared as described above to fill the entire core volume with soil. The other type was packed with soil to within 3 mm of the height of the core and the remaining volume was filled with a wet 1:1 (w/v) suspension of plaster of paris ( $\text{CaSO}_4 \cdot 0.5\text{H}_2\text{O}$ ), which was used as the core base. Preliminary tests were conducted to establish the wet (saturated) water content of the plaster base ( $1.14 \text{ kg kg}^{-1}$ ), so that this could be accounted for in later calculations. Treatments L and H were prepared in triplicate and treatment S was prepared in duplicate.

A final set of triplicate samples were prepared by filling larger cylindrical cores (50-mm i.d., 50-mm height) to just the L and H compressed states for each of the six soils, as described above. These cores were used for x-ray CT scanning.

### Soil Water Release Characteristic

The cores with the plaster bases were saturated for 48 h on a tension plate connected to a water reservoir. The water level in the reservoir was lowered progressively to give a range of matric potentials between 0 and  $-10 \text{ kPa}$ . At each potential, the soil core was weighed every 24 h until the water content did not differ significantly ( $P > 0.05$  by Student's  $t$ -test) between successive daily measurements. The plaster base reestablished hydraulic contact between the soil and the tension plate between measurements (Townend et al., 2001). The other set of cores were saturated as described above and then equilibrated at a range of matric potentials between  $-13$  to  $-1500 \text{ kPa}$  in a pressure plate apparatus for 28 d. At equilibration, the wet soil weight was recorded and the total soil volume was estimated by measuring the height and diameter with the displacement measurement system of a loading test frame and digital calipers, respectively. Water contents were calculated following oven drying at  $105^\circ\text{C}$  for 48 h.

### X-Ray Computed Tomography Scanning

The cores were placed individually in an HMX ST CT scanner (X-Tek Systems Ltd, Tring, UK). A set of digital radiographs on a gray scale were created at a voxel resolution of  $30 \mu\text{m}$  as the core was rotated about its vertical axis. From the gray-scale images, a representative set of 100 adjacent vertical “slices” of a cross-sectional area of 32 by 21 mm was selected, and this was converted to a set of binary solid (white) and pore (black) images by a thresholding process. The total porosity  $>30 \mu\text{m}$  was calculated by expressing the pore area as a proportion of the total area in the set of 100 slices.

### Statistical Analysis

All the statistical analysis reported here was performed with GenStat 12 (VSN Int. Ltd, Hemel Hempstead, UK). We used Student's  $t$ -tests to monitor equilibration during the soil water release characteristic experiments. The FITNONLINEAR directive was used to derive models of the characteristic and to express the degree of saturation as a function of matric potential and porosity. For the purposes of modeling, we used the modulus of matric potential to convert the units to positive values. The key indices of goodness-of-fit were the MSE and the proportion of the variance accounted for by the fit ( $R^2_{\text{adj}}$ ), which is the difference between 1 and the ratio of the MSE and the mean of the total sum-of-squares (total variance). The  $R^2_{\text{adj}}$  value has the advantage over the conventional squared coefficient of correlation ( $R^2$ ) in that it takes into account the number of parameters in the model. We used ANOVA to examine the effect of the structural conditions and we report the  $F$ -test probability as  $P$  by convention.

## RESULTS

### Water Content–Consolidation Characteristic

For all soils, the density achieved by the constant load increased with increasing water content up to a certain point, beyond which the density declined (Fig. 1). The water content at maximum density was derived from the fitted polynomial function. This water content was similar for the three arable soils but greater for the grassland soils, particularly Rowden (Table 1).

### Soil Water Release Characteristic

Water release characteristics expressed on a gravimetric basis for the L and H compressed soils are shown in Fig. 2. The water contents of the L treatment were significantly greater than those of the H treatment ( $P < 0.01$  by ANOVA) for all soils except Bridestowe ( $P = 0.617$ ). The ANOVA also revealed a significant interaction between compression and matric potential ( $P < 0.001$ ) in all soils except the Broadbalk (P)KMg soil ( $P = 0.225$ ). In all soils except Broadbalk (P)KMg, the H treatment soil retained significantly less water than the L treatment soil at matric

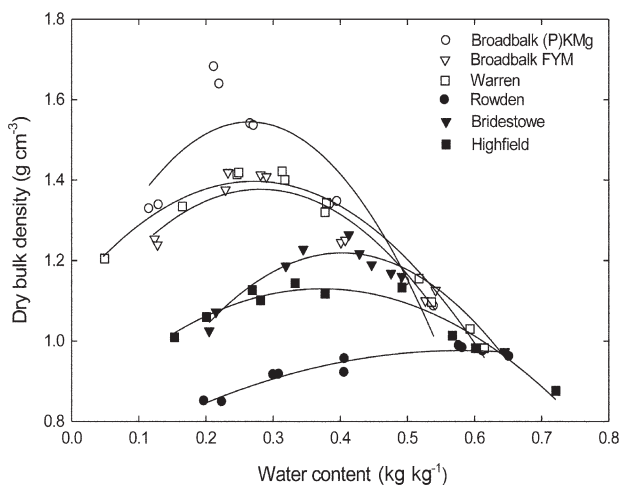


Fig. 1. The water content–density characteristic of the six soils under a constant 200-kPa compression stress fitted with second-order polynomial functions (lines).

potentials between 0 and  $-0.5$  kPa ( $P < 0.05$ ), whereas differences at matric potentials less than  $-2$  kPa were not significant.

Gravimetric water release characteristics can be used to explore the modality of soil pore size distributions (Dexter et al., 2008). We fitted the sum of two functions to our L compressed soil data set (Fig. 2) in a similar exercise to that described previously by others (e.g., Ross and Smettem, 1993; Durner, 1994). With the Mualem constraint of  $m = 1 - 1/n$ , we fitted the sum of two van Genuchten functions (van Genuchten, 1980):

$$\theta_{\psi(g)} = \left\{ \theta_{rh} + \frac{\theta_{sh} - \theta_{rh}}{\left[ 1 + (\alpha_h \psi)^{n_h} \right]^{1-(1/n_h)}} \right\} + \left\{ \theta_{rl} + \frac{\theta_{sl} - \theta_{rl}}{\left[ 1 + (\alpha_l \psi)^{n_l} \right]^{1-(1/n_l)}} \right\} \quad [1]$$

where  $\theta_s$  and  $\theta_r$  are the saturated and residual gravimetric water contents, respectively,  $\theta_{\psi(g)}$  is the gravimetric water content at matric potential  $\psi$  (kPa), i.e., the absolute value), and  $\alpha$  and  $n$  are fitted parameters. Water release at high (near-saturation) and low (drained) matric potentials are indicated by the subscripts  $h$  and  $l$ , respectively. The fitted parameters were calculated by least squares. Table 2 shows the parameters of both Eq. [1] and those of a single van Genuchten function fitted to the same data. Figure 2 shows the fit of Eq. [1] to the L experimental data (solid line) as well as the two separate components of Eq. [1] (dashed and dotted lines). We found that the goodness-of-fit was very similar between a single and a double van Genuchten function (Table 2); however, the component in Eq. [1] representing water release at lower (more negative) matric potentials,

$$\theta_{\psi(g)} = \left\{ \theta_{rl} + \frac{\theta_{sl} - \theta_{rl}}{\left[ 1 + (\alpha_l \psi)^{n_l} \right]^{1-(1/n_l)}} \right\} \quad [2]$$

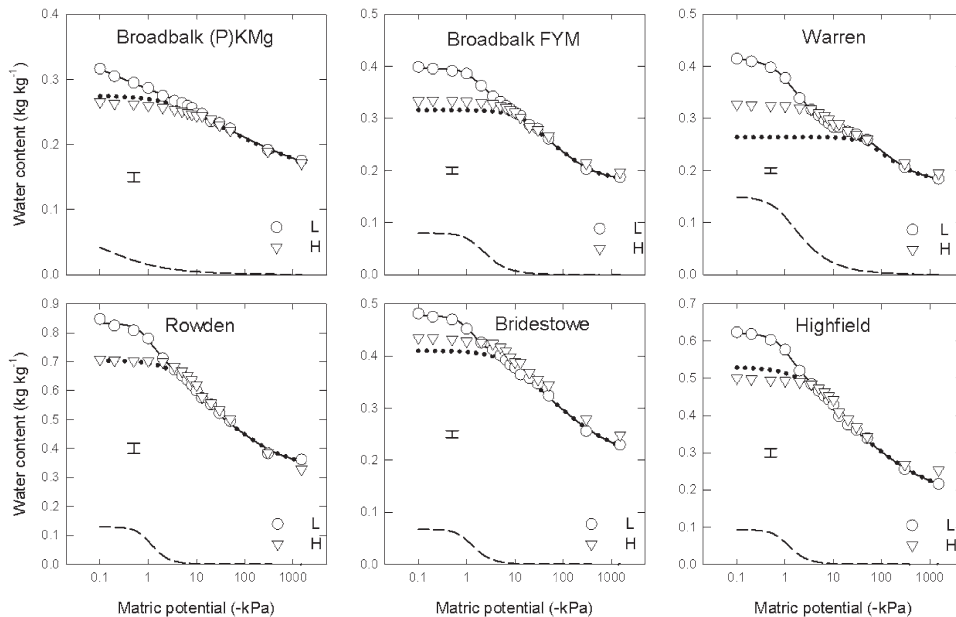


Fig. 2. Gravimetric soil water release characteristics of the six soils in the 50- (L) and 200-kPa (H) compressed structural states. The L compressed soil data were fitted with the sum of two component van Genuchten functions (solid line): one function shows the water release component associated with high (near-saturation) matric potentials (dashed line) and the other function shows the water release component associated with low (more negative) matric potentials (dotted line). Function parameters are listed in Table 2. The bar gives the standard error of the difference (SED) [ $P < 0.001$  except for Broadbalk (P)KMg ( $P = 0.225$ ) and Rowden ( $P = 0.009$ );  $df = 64$ ] for the structural state  $\times$  matric potential interaction within a soil. Note the different y-axis scales for the soils.

gave a reasonable prediction of the H compressed soil water release characteristic (obtained when fitting Eq. [1]) for most soils (see Fig. 2, dotted lines). For Broadbalk FYM and the three grassland soils,  $>80\%$  of the variation in the H water release characteristic was explained by the low matric potential component function of Eq. [1] (i.e., Eq. [2]; Table 2).

Water release characteristics expressed on a volumetric basis are shown in Fig. 3. As a main treatment effect for all soils, the S treatment resulted in a significantly greater water content than the compressed soils ( $P < 0.05$  by ANOVA). Furthermore, the H compression treatment had a significantly greater water content than the L treatments ( $P < 0.05$ ) for all soils except Broadbalk (P)KMg. The interaction between structural condition and matric potential was significant ( $P < 0.001$ ) in all soils except Broadbalk (P)KMg soil ( $P = 0.341$ ).

We fitted the van Genuchten function with the Mualem constraint to the soil water release characteristic data:

$$\theta_{\psi(v)} = \left\{ \theta_r + \frac{\theta_s - \theta_r}{\left[ 1 + (\alpha \psi)^n \right]^{1-(1/n)}} \right\} \quad [3]$$

where  $\theta_s$ ,  $\theta_r$ , and  $\theta_{\psi(v)}$  are the saturated, residual, and  $\psi$  matric potential (kPa) volumetric water contents ( $\text{m}^3 \text{m}^{-3}$ ), respectively, and  $\alpha$  and  $n$  are fitting parameters. The fit and the parameters are shown in Fig. 3 and Table 3. The fits were significant and accounted for most of the variance. Note that our measurements have already taken the volume change into account and so we used the van Genuchten function as a simple conventional model to describe our data.

## The Relationship between Water Release and Volume Change

We wanted to see if a single expression could successfully predict the saturation state of a soil as a function of matric potential and porosity in an approach similar to that of Gallipoli et al. (2003). They modified the van Genuchten function by replacing the  $\alpha$  term with  $a e^b$  where  $e$  is the void ratio and  $a$  and  $b$  are fitted parameters. We simplified the model by using the Mualem constraint and by removing  $a$ , which we found to be highly correlated with  $b$  (correlation of 0.970–0.996), to give a two-parameter function:

$$S = \frac{1}{\left[ 1 + (\varepsilon^b \psi)^n \right]^{1-(1/n)}} \quad [4]$$

where  $S$  is the degree of saturation,  $\varepsilon$  is porosity (correlated to  $e$ ), and  $b$  and  $n$  are fitted parameters. The values of

$\epsilon$  we used were those that we directly measured, as amended by the initial structural state and subsequent shrinkage during water release. We tried to fit a common model for each soil to describe the relationship between  $S$ ,  $\psi$ , and  $\epsilon$  for all three structural conditions (L, H, and S), but only 28 to 63% of the variance could be accounted for at  $P < 0.001$  (Table 4). When the  $b$  parameter was allowed to vary according to the initial structural state, the goodness-of-fit increased considerably and for four of the soils >90% of the variance was accounted for. Parameter  $b$  increased with the severity of the initial deformation process, and similar values were recorded for this parameter at the H compressed and S sheared conditions for all three grassland soils and the Broadbalk FYM arable soil. The value of  $n$  was similar for all soils.

Most agricultural soils have a sizable residual water content at low matric potentials (e.g., -1500 kPa) so we also fitted the following:

$$S = \left\{ \frac{S_m - S_r}{\left[ 1 + (\epsilon^b \psi)^n \right]^{1-(1/n)}} \right\} + S_r \quad [5]$$

where  $S_r$  is the residual saturation and  $S_m$  is the maximum saturation. The goodness-of-fit was improved slightly with this approach due to the two extra fitted parameters (Table 4). The value of  $S_r$  was generally greater for the arable soils than the grassland soils, and  $S_m$  was close to 1 for all soils.

The shrinkage characteristics measured during the water release characteristic are given in Fig. 4. Remolded S soils had a large normal shrinkage phase (i.e., close to the 1:1 line in Fig. 4), particularly in the Broadbalk FYM, Bridestowe, and Highfield soils. The two compressed soils show residual shrinkage tendencies (Haines, 1923), where the shrinkage of the pore volume was less than the volume of water released at low water contents. The L compressed soils tended to have a pronounced initial phase at high water content where the volume of water loss was much greater than the shrinkage, defined as structural shrinkage (Stirk, 1954).

### X-Ray Computed Tomography Scanning

Representative scans of the initial condition of the six soils in L and H compressed structural states are shown in Fig. 5, and mean porosity >30  $\mu\text{m}$  (the resolution of the scan) is shown in Table 5. Compression H significantly

reduced porosity in all six soils ( $P < 0.05$  by ANOVA) compared with the L compressed state, and the images suggest that this loss mainly occurred in the larger interaggregate pores. The Broadbalk FYM, Rowden, and Highfield soils were the most porous in the 50-kPa compression state.

## DISCUSSION

### The Effect of Compression

The gravimetric water release characteristic data are useful for exploring the dual porous nature of soil (e.g., Dexter et al., 2008). This showed that the effect of the two compression treatments was reflected in differences in water content between 0 and -10 kPa matric potential but not at lower (more negative) potentials (Fig. 2). At -10 kPa matric potential, the pores that have drained are those approximately >30  $\mu\text{m}$  in diameter. Hence the pores most affected by the compression were those >30  $\mu\text{m}$  in size. Interestingly, the resolution of the CT scans was also 30  $\mu\text{m}$  and these confirmed a considerable loss of >30- $\mu\text{m}$  interaggregate porosity as the compression stress increased from 50 to

**Table 2. Parameters of the van Genuchten function, with the Mualem constraint, of gravimetric water content [ $\theta_{\psi(g)}$  in  $\text{kg kg}^{-1}$ ] in 50-kPa compressed soil as a function of matric potential ( $\psi$ , in  $|\text{kPa}|$ ) for the six soils, as shown in Fig. 2, where  $\theta_s$  and  $\theta_r$  are the saturated and residual gravimetric water contents, respectively, and  $\alpha$  and  $n$  are fitted parameters. The data were fitted with either a single function (single) (df = 44) or as the sum of two component functions (df = 41): one function describes the water release component associated with high (near-saturation) matric potentials (high  $\psi$ ) and the other function describes the water release component associated with low (more negative) matric potentials (low  $\psi$ ). The low matric potential water release component was then fitted to the 200-kPa compressed soil data (df = 44). The MSE is the mean square error and the  $R^2_{\text{adj}}$  value gives the proportion of the variance accounted for by the fit.**

Soil	van Genuchten function fitted	Indicators of goodness-of-fit		van Genuchten function parameters:			
		MSE	$R^2_{\text{adj}}$	$\theta_s$	$\theta_r$	$\alpha$	$n$
Broadbalk (P)KMG	single	$1.93 \times 10^{-4}$	0.877	0.317	0.000	3.111	1.070
	two: high $\psi$	$2.03 \times 10^{-4}$	0.870	0.055	0.000	11.420	1.517
	low $\psi$			0.275	0.084	0.298	1.123
	low $\psi$ to 200 kPa	$2.75 \times 10^{-4}$	0.690				
Broadbalk FYM	single	$2.88 \times 10^{-4}$	0.931	0.421	0.000	2.453	1.097
	two: high $\psi$	$2.39 \times 10^{-4}$	0.942	0.080	0.000	0.574	2.349
	low $\psi$			0.316	0.172	0.042	1.572
	low $\psi$ to 200 kPa	$3.88 \times 10^{-4}$	0.803				
Warren	single	$2.94 \times 10^{-4}$	0.935	0.437	0.000	5.473	1.100
	two: high $\psi$	$2.50 \times 10^{-4}$	0.945	0.150	0.000	0.970	1.824
	low $\psi$			0.264	0.177	0.011	1.914
	low $\psi$ to 200 kPa	$1.96 \times 10^{-3}$	–				
Rowden	single	$1.37 \times 10^{-3}$	0.937	0.849	0.211	1.098	1.205
	two: high $\psi$	$1.45 \times 10^{-3}$	0.933	0.129	0.000	1.025	2.917
	low $\psi$			0.704	0.297	0.172	1.353
	low $\psi$ to 200 kPa	$1.73 \times 10^{-3}$	0.881				
Bridestowe	single	$2.51 \times 10^{-4}$	0.952	0.484	0.000	1.102	1.102
	two: high $\psi$	$2.59 \times 10^{-4}$	0.951	0.067	0.000	0.924	2.735
	low $\psi$			0.410	0.168	0.089	1.288
	low $\psi$ to 200 kPa	$5.91 \times 10^{-4}$	0.812				
Highfield	single	$7.63 \times 10^{-4}$	0.949	0.633	0.096	1.116	1.203
	two: high $\psi$	$8.07 \times 10^{-4}$	0.947	0.093	0.000	1.015	2.763
	low $\psi$			0.529	0.124	0.288	1.247
	low $\psi$ to 200 kPa	$7.50 \times 10^{-4}$	0.886				

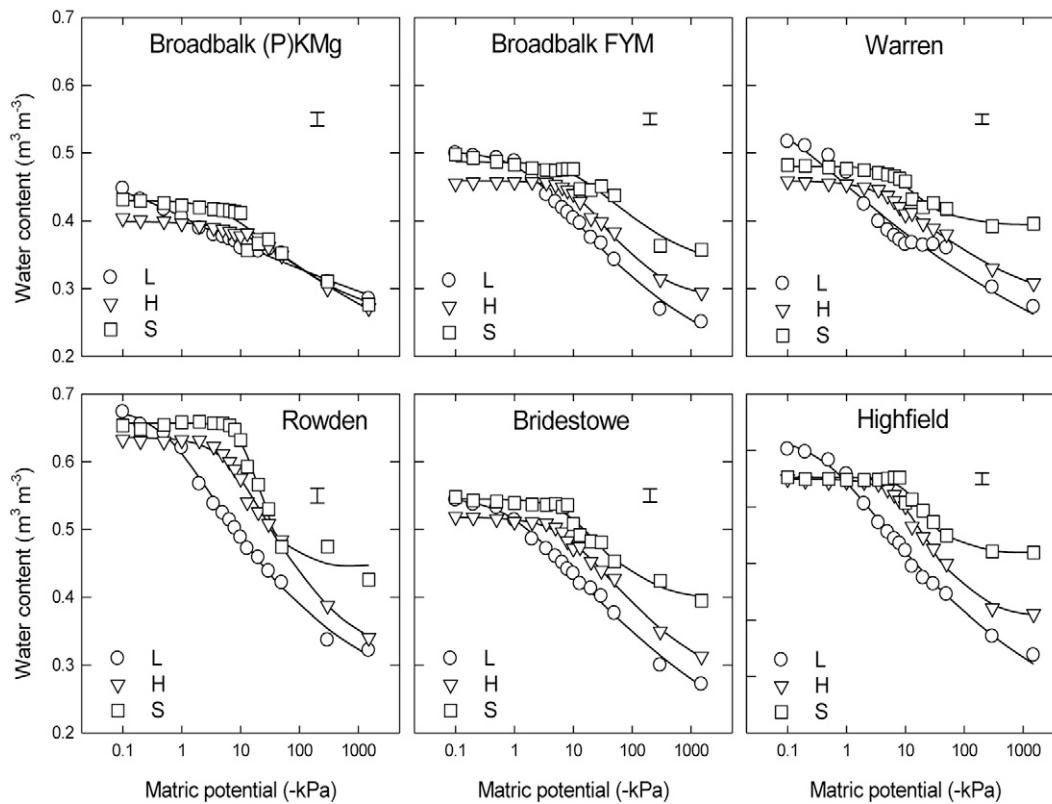


**Fig. 3.** Volumetric soil water release characteristics of the six soils in the 50-kPa compressed (L), 200-kPa compressed (H), and shear deformed (S) initial structural states fitted with van Genuchten functions (lines). Function parameters are listed in Table 3. The bar gives the standard error of the difference (SED) [ $P < 0.001$  except for Broadbalk (P)KMg ( $P = 0.341$ );  $df = 30$ ] for the structural state  $\times$  matric potential interaction within a soil.

**Table 3.** Parameters of the van Genuchten function, with the Mualem constraint, of volumetric water content [ $\theta_{\psi(v)}$ , in  $m^3 m^{-3}$ ] as a function of matric potential ( $\psi$ , in  $|kPa|$ ) for the six soils in the 50-kPa compressed (L) ( $df = 44$ ), 200-kPa compressed (H) ( $df = 44$ ), and shear deformed (S) ( $df = 28$ ) initial structural states, as shown in Fig. 3, where  $\theta_s$  and  $\theta_r$  are the saturated and residual volumetric water contents, respectively, and  $\alpha$  and  $n$  are fitted parameters. The MSE is the mean square error and the  $R^2_{adj}$  value gives the proportion of the variance accounted for by the fit.

Soil	Structural state	Indicators of goodness-of-fit		van Genuchten function parameters:			
		MSE	$R^2_{adj}$	$\theta_s$	$\theta_r$	$\alpha$	$n$
Broadbalk (P)KMg	L	$4.38 \times 10^{-4}$	0.780	0.461	0.000	15.000	1.046
	H	$2.60 \times 10^{-4}$	0.831	0.399	0.080	0.084	1.108
	S	$2.79 \times 10^{-4}$	0.874	0.430	0.229	0.130	1.261
Broadbalk FYM	L	$1.81 \times 10^{-4}$	0.968	0.502	0.109	0.558	1.158
	H	$1.86 \times 10^{-4}$	0.932	0.459	0.275	0.058	1.510
	S	$3.76 \times 10^{-4}$	0.806	0.487	0.303	0.071	1.289
Warren	L	$4.75 \times 10^{-4}$	0.905	0.556	0.000	15.000	1.075
	H	$9.05 \times 10^{-5}$	0.955	0.459	0.241	0.203	1.209
	S	$1.33 \times 10^{-4}$	0.870	0.480	0.394	0.117	1.930
Rowden	L	$3.37 \times 10^{-4}$	0.969	0.678	0.199	1.478	1.185
	H	$4.00 \times 10^{-4}$	0.945	0.636	0.282	0.108	1.347
	S	$4.37 \times 10^{-4}$	0.937	0.657	0.447	0.061	2.548
Bridestowe	L	$3.29 \times 10^{-4}$	0.947	0.547	0.000	1.012	1.097
	H	$2.67 \times 10^{-4}$	0.930	0.518	0.208	0.107	1.216
	S	$2.84 \times 10^{-4}$	0.879	0.545	0.390	0.091	1.547
Highfield	L	$3.15 \times 10^{-4}$	0.973	0.621	0.000	2.057	1.128
	H	$4.12 \times 10^{-4}$	0.936	0.549	0.297	0.088	1.642
	S	$2.70 \times 10^{-4}$	0.891	0.552	0.419	0.068	2.188

200 kPa (Fig. 5). When the L compressed soil data were fitted with the sum of two van Genuchten functions (Ross and Smettem, 1993; Durner, 1994), the function describing the smaller intraaggregate pores gave a good prediction of the water release characteristic of the H compressed soil (Fig. 2, dotted lines). The CT scans showed very little  $>30\text{-}\mu\text{m}$  pore space within aggregates (Fig. 5), even in the less-compressed soil treatment, and hence we can infer that the intra-aggregate pores least affected by the compression were  $<30\text{ }\mu\text{m}$  in size.

The water release and CT scan data sets therefore appear to be in agreement as to the effect of the compression treatment. Dexter et al. (2008) and Matthews et al. (2010) demonstrated

a similar effect of compaction on larger structural pores. Richard et al. (2001) found that a 90-kPa compaction treatment in a wet soil reduced the volume of pores in the 15- to 60- $\mu\text{m}$  range. Li and Zhang (2009) reported decreases in interaggregate pores 2 to 70  $\mu\text{m}$  in size with compaction and resistance of smaller pores to compression. In these discussions, however, we need to reiterate that our experiments were conducted under controlled conditions on repacked soils where the inherent field structure had been disturbed. Thus the nature of the interaggregate porosity may not necessarily reflect real field conditions. We can speculate that the smaller intraaggregate porosity was less affected by our preparations.

On a volumetric basis, the effects of compaction on the water release characteristic tended to be reflected in an increase in water content due to the increase in density, as has been reported previously (e.g., Wu et al., 1997; Richard et al., 2001; Gregory et al., 2009).

## The Effect of Shear Deformation

The S remolded soil retained more water than the H compressed soil (Fig. 3). The structural condition in these soils was created by shearing and remolding the soil when it was in a plastic state. We postulate that this preparation collapsed the largest pores and created more of the smaller water-retaining pores by proportion. An exception to this was the Broadbalk (P)KMg soil, where the three curves were similar (Fig. 3). The magnitude of the difference in water retention at high (near-saturation) matric potentials between the H compressed and S remolded soil treatments appeared to be less than that between the L and H compressed treatments. As shear deformation represents a worst-case structure-damaging process, this may suggest that the H compressed treatment also had quite a considerable damaging effect, particularly on the larger soil pores.

## Shrinkage Characteristics

Shrinkage was greater in sheared soils than compressed soils (Fig. 4). This is consistent with collapse of the matrix into small pores. The important implication is that the remolded soils remained tension saturated, even at very low matric potentials, due to normal shrinkage. This supports the work of others who have linked normal shrinkage to the collapse of larger interaggregate pores and a greater proportion of finer intraaggregate pores (Newman and Thomasson, 1979; Bronswijk, 1991; Cabidoche and Ozier-Lafontaine, 1995; Li and Zhang, 2009).

The compressed soils did not shrink to the same extent as the sheared soils. Some of the L compressed soils in particular showed structural shrinkage initially where water was presumably released from the largest interaggregate pores with little volume change. Others have reported a lack of normal shrinkage in compressed soils (e.g., Wu et al., 1997).

## Modeling the Water Release Characteristics as a Function of Porosity and Matric Potential

We were interested in the volume change caused by the initial deformation in addition to shrinkage during water release

**Table 4. Parameters of degree of saturation ( $S$ ) as a function of matric potential ( $\psi$ , in |kPa|) and porosity ( $\epsilon$ ) for the six soils, where  $b$  and  $n$  are fitted parameters. A single two-parameter function describing all three initial structural states (all) ( $df = 126$ ) is given together with functions where the porosity exponential factor  $b$  was allowed to vary for 50-kPa compressed (L), 200-kPa compressed (H) and shear deformed (S) states ( $df = 124$ ). Fits of a modified four-parameter function with extra parameters  $S_m$  (maximum  $S$ ) and  $S_r$  (residual  $S$ ) are also listed ( $df = 122$ ) for the case where  $b$  was allowed to vary. The MSE is the mean square error and the  $R^2_{adj}$  value gives the proportion of the variance accounted for by the fit.**

Soil	Structural state	Parameters	Indicators of goodness-of-fit		Function parameters: $S = 1/[1 + (\epsilon^b \psi)^n]^{1-(1/n)}$ or $S = (S_m - S_r)/[1 + (\epsilon^b \psi)^n]^{1-(1/n)} + S_r$			
			MSE	$R^2_{adj}$	$n$	$b$	$S_m$	$S_r$
Broadbalk (P)KMg	all	2	$4.00 \times 10^{-3}$	0.373	1.033	0.155		
	L		$2.78 \times 10^{-3}$	0.566	1.029	-2.749		
	H					0.543		
	S					1.615		
	L	4	$2.51 \times 10^{-3}$	0.608	1.839	-0.681	0.983	0.827
	H					3.367		
Broadbalk FYM	all	2	$6.01 \times 10^{-3}$	0.569	1.100	3.238	0.995	
	L		$9.43 \times 10^{-4}$	0.932	1.099	0.902		
	H					3.883		
	S					6.647		
	L	4	$9.37 \times 10^{-4}$	0.933	1.180	1.364		0.314
	H					4.247		
Warren	all	2	$8.32 \times 10^{-3}$	0.288	1.033	-1.860		
	L		$2.49 \times 10^{-3}$	0.787	1.044	-4.548		
	H					1.019		
	S					4.874		
	L	4	$2.02 \times 10^{-3}$	0.827	1.494	-0.832	0.974	0.692
	H					3.534		
Rowden	all	2	$7.86 \times 10^{-3}$	0.633	1.109	3.216		
	L		$1.38 \times 10^{-3}$	0.936	1.095	-1.964		
	H					3.582		
	S					6.476		
	L	4	$1.30 \times 10^{-3}$	0.939	1.187	-1.255	1.007	0.346
	H					4.040		
Bridestowe	all	2	$7.04 \times 10^{-3}$	0.565	1.090	2.779		
	L		$1.20 \times 10^{-3}$	0.926	1.016	0.353		
	H					3.373		
	S					7.800		
	L	4	$1.20 \times 10^{-3}$	0.926	1.142	0.790	0.995	0.226
	H					3.743		
Highfield	all	2	$1.25 \times 10^{-2}$	0.535	1.117	2.576		
	L		$1.85 \times 10^{-3}$	0.931	1.115	-1.130		
	H					3.241		
	S					7.871		
	L	4	$1.71 \times 10^{-3}$	0.936	1.293	0.233	0.994	0.384
	H					4.047		
	S				8.880			

in agricultural soils. We found that we could explain 28 to 63% of the variance in saturation, irrespective of the initial structural damage to the soil. It seems that when the porosity exponential factor  $b$  varies in a systematic way (i.e., it increases with the degree of soil damage), a much better fit to the data can be obtained. The adjustment of  $b$  has the effect of shifting the inflection point of the water release characteristic to lower (more negative) matric

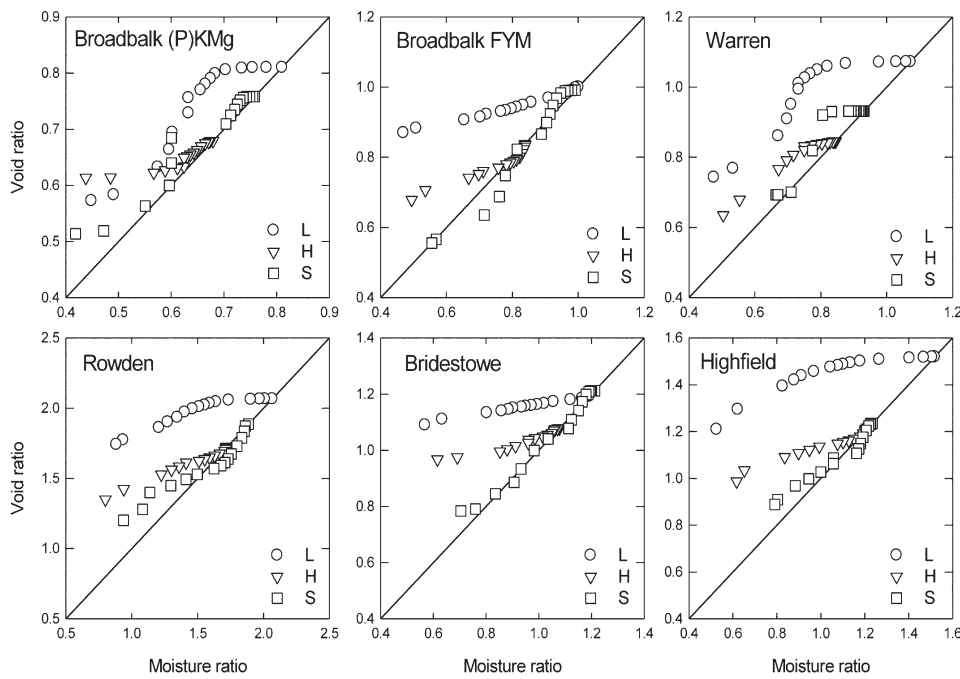


Fig. 4. Shrinkage characteristics of the six soils in the 50-kPa compressed (L), 200-kPa compressed (H), and shear deformed (S) initial structural states. The line shows 1:1 normal shrinkage where changes in water volume (moisture ratio) are equal to changes in pore volume (void ratio). Note the different axis scales for the soils.

potentials. The variation in *b* between treatments was sufficiently systematic to provide scope to develop a more general model of the effects of soil damage on the water release characteristic.

### Differences in the Response of the Different Soils

The grassland soils were generally more porous than the arable soils (Fig. 5) and released more water across the range of matric potentials in this study (Fig. 2 and 3). Notwithstanding the possible discontinuity between the structure in the field and that recreated in the laboratory, this suggests that the grassland soils had a greater range of component pore sizes, which was undoubtedly due in part to the greater soil OM content. The effect of long-term incorporation of farm-yard manure was reflected in differences in the porosity and physical behavior between the Broadbalk FYM and (P)KMg soils, as has been found previously (Matthews et al., 2010). These soils have exactly the same particle size distribution but differ in soil OM content (Table 1).

This further illustrates the interaction between soil structure, soil OM, and resilience to stress. The soil OM is a key component in the development and stabilization of soil structure, which in turn

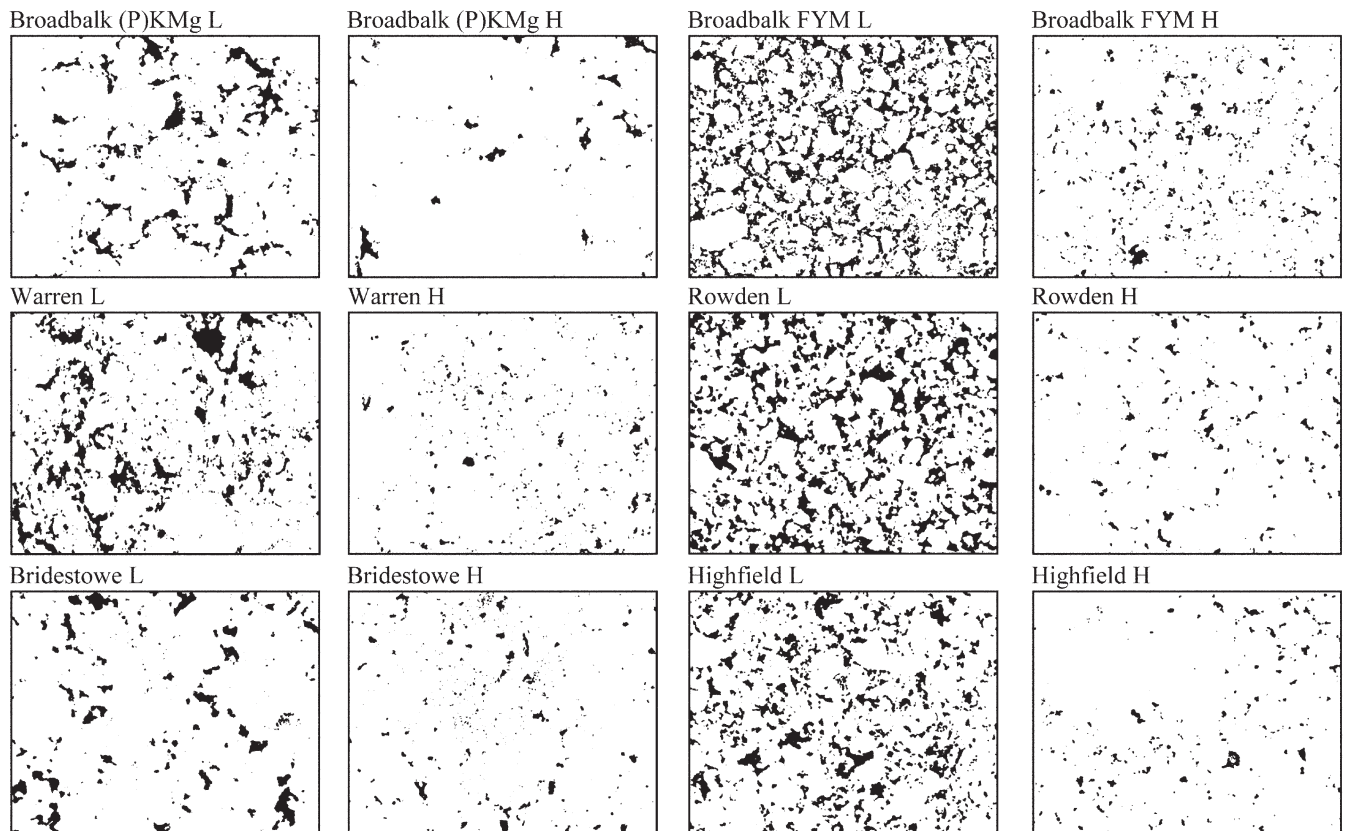


Fig. 5. Binary x-ray computed tomography scans of the six soils in the 50-kPa compressed (L) and 200-kPa compressed (H) initial structural states as prepared for the soil water release characteristic showing solid (white) and pore (black) space. Each image is 32- by 21-mm in size and the pixel resolution is 30  $\mu\text{m}$ .

provides interaggregate habitat space for soil microbial communities and intraaggregate protection of OM from degradation, thus increasing soil C pools. Gregory et al. (2009) found that grassland soils were more resilient to both physical and biological stresses than arable soils in a study that included some of the soils tested here (Broadbalk FYM, Warren, and Highfield).

## CONCLUSIONS

Increasing the severity of compression mainly affected the larger pores, resulting in a change from a dual-porosity system of inter- and intraaggregates to one mainly dominated by smaller intraaggregate pores. Remolding soils when plastic had more of a severe effect than compression and affected smaller pores in addition. These soils remained tension saturated at very low matric potentials due to shrinkage within a matrix of smaller pores. For each soil, the degree of saturation was modeled as a function of matric potential and porosity, with one of the fitted parameters scaled according to antecedent soil damage. These results provide insights into the saturation status of a soil during water release based on the changes in porosity caused by structural damage and shrinkage, which is important for predicting the soil behavior. We have demonstrated the potential of a new model to describe the relationship between matric potential, saturation, and porosity.

## ACKNOWLEDGMENTS

This research was funded by the UK Biotechnology and Biological Sciences Research Council (BBSRC) with competitive grants BB/E001580/1 and BB/E001793/1. Rothamsted Research is an institute of the BBSRC. We thank Dr D.A.L. Holtham (North Wyke Research) for arranging the soil sampling from the Devon sites, Ms. A. Arguello (University of Abertay) for carrying out the x-ray CT scanning, and Mr. R.P. White (Rothamsted Research) for advice on the statistical analysis.

## REFERENCES

Avery, B.W. 1980. Soil classification for England and Wales (higher categories). Tech. Monogr. 14. Soil Surv. of England and Wales, Harpenden, UK.

Braudeau, E., M. Sene, and R.H. Mohtar. 2005. Hydrostructural characteristics of two African tropical soils. *Eur. J. Soil Sci.* 56:375–388.

Bronswijk, J.J.B. 1991. Drying, cracking, and subsidence of a clay soil in a lysimeter. *Soil Sci.* 152:92–99.

Cabidoche, Y.M., and H.O. Ozier-Lafontaine. 1995. THERESA: I. Matric water content measurements through thickness variations in Vertisols. *Agric. Water Manage.* 28:133–147.

Clayden, B., and J.M. Hollis. 1984. Criteria for differentiating soil series. Tech. Monogr. 17. Soil Surv. of England and Wales, Harpenden, UK.

Dexter, A.R., E.A. Czyz, G. Richard, and A. Reszkowska. 2008. A user-friendly water retention function that takes account of the textural and structural pore spaces in soil. *Geoderma* 143:243–253.

Durner, W. 1994. Hydraulic conductivity estimation for soils with heterogeneous pore structure. *Water Resour. Res.* 30:211–223.

Gallipoli, D., S.J. Wheeler, and M. Karstunen. 2003. Modelling the variation of degree of saturation in a deformable unsaturated soil. *Geotechnique* 53:105–112.

Gregory, A.S., C.W. Watts, B.S. Griffiths, P.D. Hallett, H.L. Kuan, and A.P. Whitmore. 2009. The effect of long-term soil management on the physical and biological resilience of a range of arable and grassland soils in England. *Geoderma* 153:172–185.

**Table 5. Total porosity (mean and standard error of the mean [SEM]) >30 µm derived from binary x-ray computed tomography scans of the six soils in the 50-kPa compressed (L) and 200-kPa compressed (H) initial structural states. The ANOVA results are expressed as the P score and the standard error of the difference (SED) between the two structural states within each soil (df = 4).**

Soil	Structural state	Porosity >30 µm		Difference between structural states	
		Mean	SEM	P	SED
Broadbalk (P)KMg	L	0.103	0.017	0.008	0.018
	H	0.012	0.006		
Broadbalk FYM	L	0.279	0.036	0.003	0.036
	H	0.049	0.005		
Warren	L	0.131	0.018	0.007	0.018
	H	0.037	0.005		
Rowden	L	0.182	0.038	0.026	0.039
	H	0.048	0.009		
Bridestowe	L	0.055	0.004	0.004	0.006
	H	0.022	0.004		
Highfield	L	0.172	0.019	0.002	0.020
	H	0.033	0.006		

Haines, W.B. 1923. The volume changes associated with variations of water content in soil. *J. Agric. Sci.* 13:296–311.

Kim, D.J., R.A. Jaramillo, M. Vauclin, J. Feyen, and S.I. Choi. 1999. Modeling of soil deformation and water flow in a swelling soil. *Geoderma* 92:217–238.

Li, X., and L.M. Zhang. 2009. Characterization of dual-structure pore-size distribution of soil. *Can. Geotech. J.* 46:129–141.

Mathews, G.P., G.M. Laudone, A.S. Gregory, N.R.A. Bird, A.G. de G. Mathews, and W.R. Whalley. 2010. Measurement and simulation of the effect of compaction on the pore structure and saturated hydraulic conductivity of grassland and arable soil. *Water Resour. Res.* (in press), doi:10.1029/2009WR007720.

Mualem, Y. 1976. A new model for predicting the hydraulic conductivity of unsaturated porous media. *Water Resour. Res.* 12:513–522.

Newman, A.C.D., and A.J. Thomasson. 1979. Rothamsted studies of soil structure: III. Pore size distributions and shrinkage processes. *J. Soil Sci.* 30:415–439.

Richard, G., I. Cousin, J.F. Sillon, A. Bruand, and J. Gueric. 2001. Effect of compaction on the porosity of a silty soil: Influence on unsaturated hydraulic properties. *Eur. J. Soil Sci.* 52:49–58.

Ross, P.J., and K.R.J. Smettem. 1993. Describing soil hydraulic properties with sums of simple functions. *Soil Sci. Soc. Am. J.* 57:26–29.

Simms, P.H., and E.K. Yanful. 2001. Measurement and estimation of pore shrinkage and pore distribution in a clayey till during soil-water characteristic curve tests. *Can. Geotech. J.* 38:741–754.

Stirk, G.B. 1954. Some aspects of soil shrinkage and the effect of cracking upon water entry into the soil. *Aust. J. Agric. Res.* 5:279–290.

Tarantino, A., and S. Tombolato. 2005. Coupling of hydraulic and mechanical behaviour in unsaturated compacted clay. *Geotechnique* 55:307–317.

Townend, J., M.J. Reeve, and A. Carter. 2001. Water release characteristic. p. 95–140. *In* K.A. Smith and C.E. Mullins (ed.) *Soil and environmental analysis: Physical methods*. 2nd ed. Marcel Dekker, New York.

van Genuchten, M.Th. 1980. A closed-form equation for predicting the hydraulic conductivity of unsaturated soils. *Soil Sci. Soc. Am. J.* 44:892–898.

Whalley, W.R., C.W. Watts, A.S. Gregory, S.J. Mooney, L.J. Clark, and A.P. Whitmore. 2008. The effect of soil strength on the yield of wheat. *Plant Soil* 306:237–247.

Wu, L., R.R. Allmaras, D. Gimenez, and D.M. Huggins. 1997. Shrinkage and water retention characteristic in a fine-textured Mollisol compacted under different axle loads. *Soil Tillage Res.* 44:179–194.